JVSTB Journal of Vacuum Science & Technology B

Synthesis and optical properties of ZnO–ZnS core-shell nanotube arrays

Hung-Chou Liao, Pai-Chia Kuo, Chin-Ching Lin, and San-Yuan Chen

Citation: Journal of Vacuum Science & Technology B **24**, 2198 (2006); doi: 10.1116/1.2232456
View online: http://dx.doi.org/10.1116/1.2232456
View Table of Contents: http://scitation.aip.org/content/avs/journal/jvstb/24/5?ver=pdfcov
Published by the AVS: Science & Technology of Materials, Interfaces, and Processing

Synthesis and optical properties of ZnO–ZnS core-shell nanotube arrays

Hung-Chou Liao, Pai-Chia Kuo, Chin-Ching Lin, and San-Yuan Chen[a)]
Department of Materials Science and Engineering, National Chiao Tung University, 1001 Ta-hsueh Road, Hsinchu, Taiwan, 30050 Republic of China

(Received 26 April 2005; accepted 21 June 2006; published 15 September 2006)

Heterostructured ZnO–ZnS core-shell nanotube arrays with the diameters of 50–80 nm and lengths up to 1 μm were synthesized by a two-step chemical reaction. First, the ZnO layer was grown by atomic-layer deposition. It was found that the preferred growth orientation was strongly dependent on the substrate temperature. After sulfuration conversion from arrayed ZnO nanorods, the ZnS–ZnO composite arrays can be successfully prepared, as evidenced from transmission electron microscopy. This confirms that the ZnO–ZnS core-shell nanotube-arrayed structure has been fabricated. X-ray photoelectron spectroscopy analysis indicates that the binding energy of S $2p$ is the same as that of bulk single-crystal ZnS and that the Zn $2p_{3/2}$ peak is shifted about 0.5 eV due to the formation of Zn–S bonds. Photoluminescence shows the relative-intensity ratio of ultraviolet emission (I_{UV}) to deep-level emission (I_{DLE}) for ZnO/ZnS core-shell nanotubes can be enhanced to be nine times that of original ZnO nanotubes. © *2006 American Vacuum Society.*
[DOI: 10.1116/1.2232456]

I. INTRODUCTION

One-dimension (1D) nanotubes and tubular nanomaterials have attracted much attention. Growth of 1D ZnO nanostructures including nanotubes,[1] nanowires,[2] nanorods,[3] and nanobelts[4] has been demonstrated recently. Semiconducting ZnO is one of the most important functional oxides for optoelectronics. Recently, many functional materials with arrayed nanostructures have been successful synthesized by various methods. Large-scale arrays of ZnO nanorods on Si and flexible substrates have been developed in our previous works.[5]

However, many research groups have found that the nonpassivated surface sites may act for deep-level recombination and suppress efficient luminescence, especially in ZnO nanorods grown by the chemical-solution route.[6,7] Song and Lee[8] reported that the ZnSe/ZnS core/shell nanocrystal showed a 2000% enhancement of luminescence quantum yield compared to bare ZnSe nanocrystals. As an important II-VI semiconductor, zinc sulfide (ZnS) has a wide band gap energy of 3.66 eV at room temperature.[9] The ZnO core was passivated by a wider band gap inorganic ZnS materials that could provide effective elimination of surface-related defect states and a confinement of charge carriers into the core material due to the band offset potential.

In this article, we report the synthesis of ZnO/ZnS core-shell nanotubes using anodic-aluminum oxide (AAO) templates to form arrayed ZnO nanotubes by the atomic-layer deposition (ALD) process and then sulfurated by Na_2S solution. In addition, UV photoluminescence of ordered ZnO–ZnS core-shell nanotubes arrays is also characterized.

a)Author to whom correspondence should be addressed; electronic mail: sychen@cc.nctu.edu.tw

II. EXPERIMENT

For the growth of the ZnO nanotubes by an ALD process on an AAO template, diethylzinc (DEZ) and H_2O reactant gases were alternately fed into the growth chamber with nitrogen as a carrier gas. The pressure in the reactor during deposition was kept at 0.2–0.6 torr. The ZnO film was deposited on the AAO template at 200 °C. The growth rate of ZnO film was controlled at 0.11 nm/cycle. After growth, the inner wall of ZnO nanotubes was sulfurated by 50 mL of 0.8M Na_2S solution for 12 h. The details of the sulfurating process can be referred to Ref. 10. The resulting core-shell nanotubes were then cleaned and dried in an isothermal oven at 70 °C. The morphology of ZnO–ZnS core-shell nanotubes was examined by scanning electron microscopy (SEM) (JEOL-6500F) operating at 15 kV and transmission electron microscopy (TEM) (Philips Tecnai 20) operating at 200 kV. The crystal structure was determined using x-ray diffraction (XRD) (M18XFH) with Cu $K\alpha$ radiation. Energy-dispersive x-ray spectroscopy (EDS) and x-ray photoelectron spectroscopy (XPS) equipped with Mg $K\alpha$ at 1253.6 eV at the anode were used for the composition analysis of the ZnO–ZnS core-shell nanotubes. The x-ray generator was operated at 15 kV and 300 W (20 mA). The XPS spectra were taken with an energy resolution of 0.1 eV/step, a dwell time of 50 ms, a pass energy of 35.75 eV, number of scans of 10 times. The carbon-based contamination in the spectrometer was used as the reference in the work and the binding energies were calibrated by referring to the C 1s line. Despite the apparent limitations and uncertainties associated with adventitious carbon referencing, it is the most convenient and commonly applied technique that were widely used in the published papers.[11–13] Photoluminescence measurement was performed by excitation from a 325 nm He–Cd laser at room temperature. Both ZnO nanorods and ZnS powder were used as the standards.

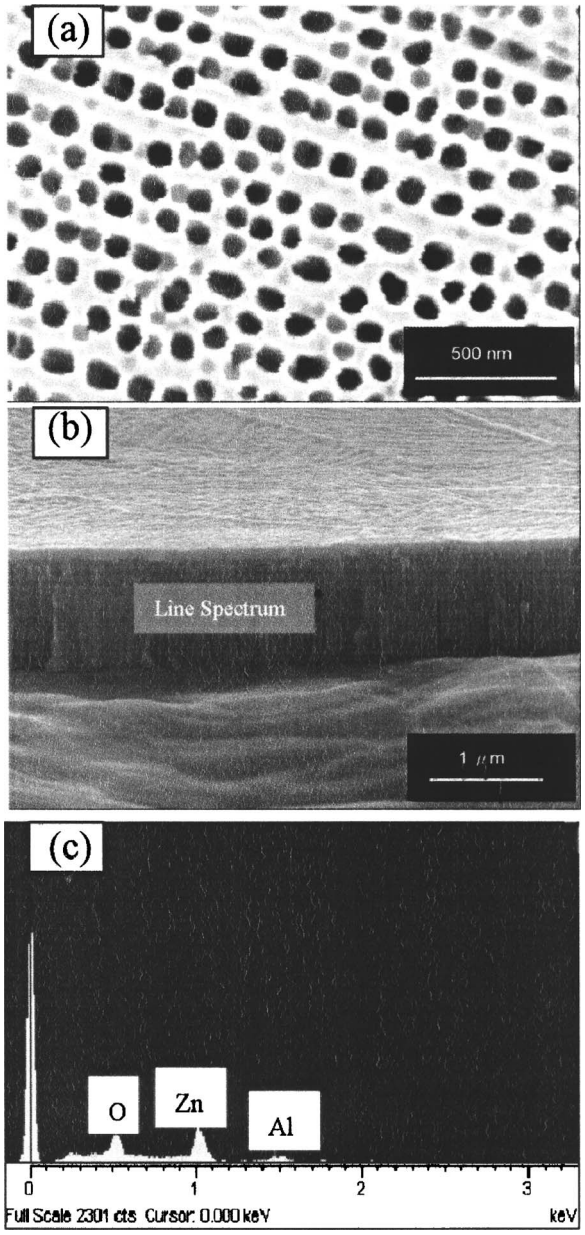

FIG. 1. SEM image of (a) AAO template and (b) ZnO nanotubes in AAO. (c) EDS spectra acquired from the side view region in (b).

III. RESULTS AND DISCUSSION

The scanning electron microscopy (SEM) images of the bare AAO and ZnO nanotube arrays in the AAO template are presented in Fig. 1. The thickness of the fabricated AAO is about 1 μm and the channel diameter is less than 100 nm. After the ZnO thin film was deposited into the channels of AAO by ALD [Fig. 1(b)], the diameter of the channel was estimated to be about 50–80 nm. EDS analysis taken from the side view ZnO nanotubes in AAO template found that the nanotubes are mainly composed of Zn and O, as shown in Fig. 1(c).

Figure 2 shows the XRD patterns obtained from ZnO nanotube arrays annealed at various substrate temperatures. It was found that the [100] orientation was first observed at

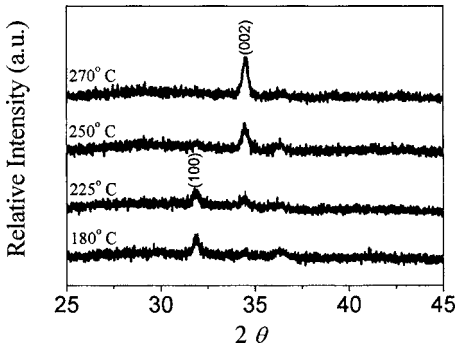

FIG. 2. XRD of ZnO nanotube arrays deposited from 180 to 270 °C.

low substrate temperatures. However, it was found that the [002] orientation would become dominant when the substrate temperature was increased above 225 °C, indicating the strong preferred orientation along the *c* axis of wurtzite ZnO. This observation suggests that the preferred growth orientation of ZnO nanotubes strongly depends on the substrate temperature and that the crystal structure of the ZnO nanotubes can be controlled.

Subsequently, the inner walls of ZnO nanotubes were sulfurated in the Na_2S solution for 12 h and it was found that the ZnO–ZnS nanotubes were formed in the AAO. Furthermore, after removing the AAO in aqueous NaOH, Fig. 3 shows the SEM image of ZnO–ZnS nanotube arrays. The nanotubes were estimated to have the average diameters of 50–80 nm and lengths of about 1 μm.

The chemical state of atoms on the surface of ZnO nanotubes was analyzed by XPS analysis. A comparison of the XPS spectra recorded from the as-synthesized ZnO nanotubes and the ZnO–ZnS core-shell nanotubes is shown in Fig. 4. The XPS analysis shows that the nanotubes are mainly composed of Zn, O, and S. The signal of S 2*p* in the ZnO nanotubes was only detected in the ZnO nanotubes with sulfurating, as illustrated in Fig. 4(a). The binding energy of S 2*p* appears at about 162.3 eV after sulfuration. This binding energy is smaller than that of sulfur-related compounds, such as elemental sulfur (164.0 eV) and chemisorbed SO_2 (163–165.5 eV).[14] This implies that the peak can be assigned to the binding energy of ZnS.[15]

Figure 4(b) shows the XPS data of Zn $2p_{3/2}$ taken from ZnO nanotubes and ZnO–ZnS core-shell nanotubes. The full

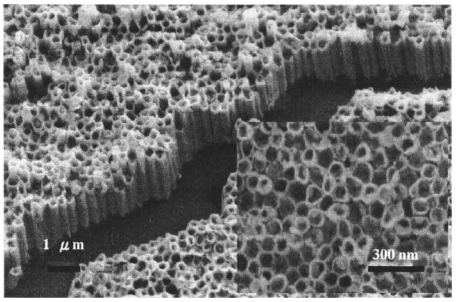

FIG. 3. SEM image of side view ZnO–ZnS core-shell nanotube arrays. Top view was shown in the inset.

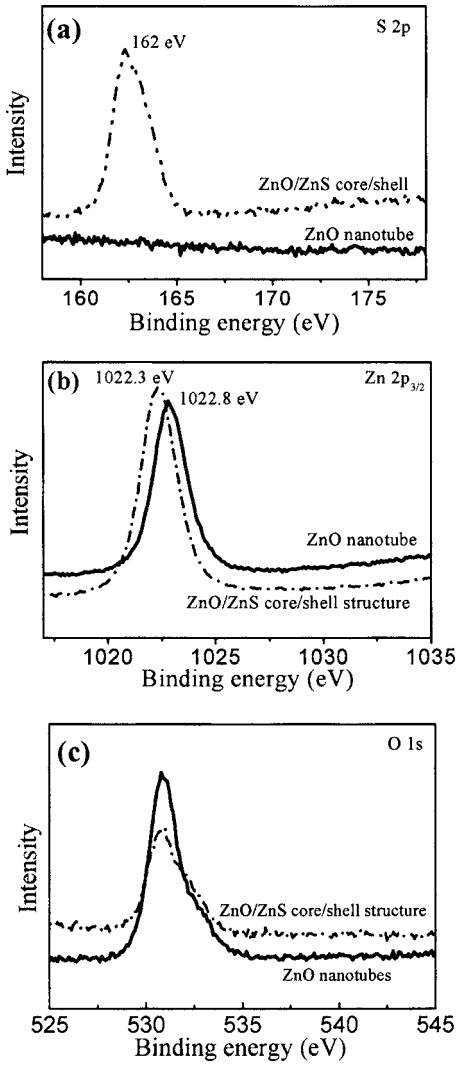

FIG. 4. XPS spectra of (a) S $2p$, (b) Zn $2p_{3/2}$, and (c) O $1s$ of ZnO and ZnO/ZnS core-shell nanotubes.

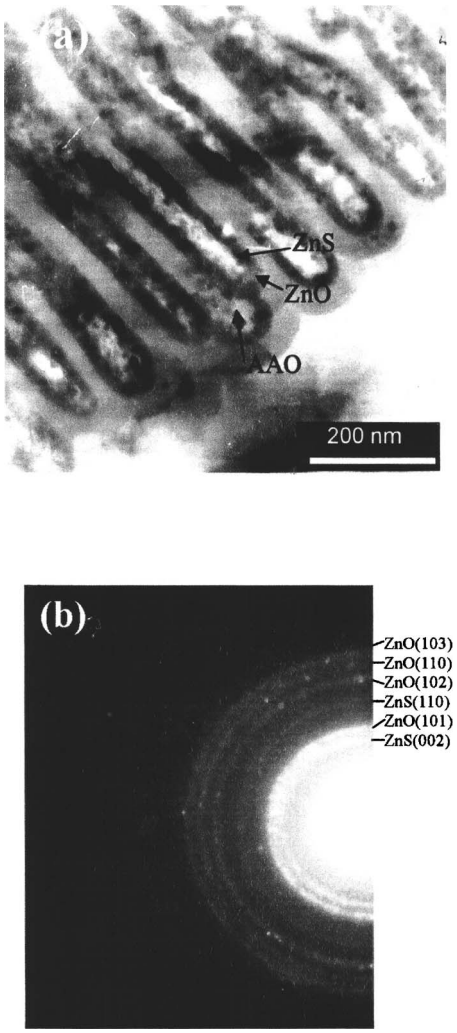

FIG. 5. (a) TEM image of ZnO–ZnS core-shell nanotubes. (b) Selected-area electron-diffraction pattern of ZnO/ZnS core-shell nanotubes, showing the presence of zinc-blende ZnS and wurtzite-structure ZnO.

width at half maximum (FWHM) of the Zn peak obtained from the ZnO nanotubes and ZnO–ZnS core-shell nanotubes are 1.578 and 1.655 eV, respectively. The Zn $2p_{3/2}$ peak obtained from the ZnO nanotubes appears to be symmetric with its peak at 1022.8 eV, which is larger than the value of Zn in bulk ZnO.[16] The measured Zn $2p_{3/2}$ spectrum of ZnO–ZnS core-shell nanotubes could be accurately fitted with two different Gaussian peak components. The XPS bonding energy spectra was fitted using computer program of XPS-PEAK4.1. The background was subtracted using Shirley's method and processed by least-square fitting with Gaussian peaks. The peaks located at 1022.8 and 1022.3 eV could be due to Zn–O bond and Zn–S bond, respectively. Figure 4(c) shows the XPS data of O $1s$ in ZnO nanotubes and ZnO–ZnS core-shell nanotubes. The asymmetric peak is possibly from some surface contamination or differential charging of the surface layer. It was found that the O $1s$ peak obtained from the ZnO–ZnS core-shell nanotubes is lower than the value of ZnO nanotubes and the difference in bonding energy between them is very small ($\sim$0.1 eV).

Figure 5(a) shows the TEM image of ZnO–ZnS core-shell nanotubes in the nanostructured AAO template. The wall thickness of the ZnS–ZnO nanotubes is roughly estimated to be about 35–50 nm. However, it was found that the ZnS surface is not smooth because the lattice constant of zinc-blende ZnS (a=0.541 09 nm) and wurtzite ZnO (a=0.3249 nm and c=0.520 65 nm) are incompatible. Furthermore, since the reaction is essentially a substitution reaction, the grown ZnS layer is also possibly a mixed ZnO–ZnS surface. Therefore, it is very difficult to measure the size of the ZnS layer on the nanosize scale by TEM images.

The selected-area electron diffraction in Fig. 5(b) recorded from the core-shell nanotube reveals two sets of ring diffraction patterns which fit very well to zinc-blende structure ZnS and wurtzite structure ZnO, indicating that polycrystalline ZnS has been grown on the ZnO nanotubes. Furthermore, this demonstrates that ZnO–ZnS core-shell nanotubes have been developed.

The photoluminescence (PL) property of the ZnO–ZnS nanostructures was measured and is shown in Fig. 6. A small

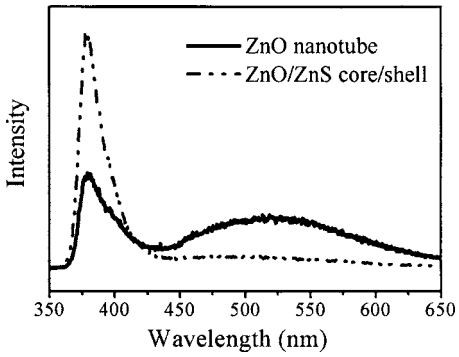

FIG. 6. PL spectra of ZnO and ZnO–ZnS core-shell nanotubes.

shift of ~1.5 nm was observed for the ZnO–ZnS nanostructure. This shift is possibly due to the reduced size of the ZnO nanotubes, especially in the wall-thickness direction of the nanotubes.[17] Moreover, it was found that the UV emission intensity of ZnO–ZnS core-shell nanotubes is stronger than that of ZnO nanotubes. The weakness in deep-level emission presumably results from the suppression of nonradiative recombination due to reduced concentrations of surface states.[18] Therefore, the relative ratio of the peak intensity of UV emission (I_{UV}) to that of deep-level emission (I_{DLE}) for ZnO–ZnS core-shell nanotubes could be enhanced nine times that of original ZnO nanotubes. A higher PL ratio implies that the ZnO–ZnS core-shell nanotubes exhibit higher optical quality and can be applied in advanced nanostructured photoelectronics.

IV. CONCLUSION

In summary, using AAO as a template, ZnO nanotubes array can be fabricated by the atomic-layer chemical-vapor-deposition technique. After the sulfurating reaction, the ZnO–ZnS core-shell nanotube arrays were synthesized. The wall thickness of ZnO–ZnS core-shell nanotubes is about 35–50 nm. A small blueshift was observed from the PL spectra of the ZnO–ZnS core-shell nanotubes, possibly caused by a small quantum-confinement effect. Moreover, this relative-intensity ratio of UV emission (I_{UV}) to deep-level emission (I_{DLE}) is much stronger for ZnO/ZnS core-shell nanotubes as compared with original ZnO nanotubes that can be attributed to the surface passivation of ZnO nanotubes by a wider band gap material, ZnS. This ratio could be enhanced by the factor of 9. The ZnO–ZnS core/shell nanostructures may have potential and useful applications in advanced nanoscale electronics, optics, and other devices.

ACKNOWLEDGMENT

The authors gratefully acknowledge the financial support of the National Science Council of Taiwan through Contract No. NSC-94-2216-E-009-016.

[1]Y. J. Xing, Z. H. Xi, Z. Q. Xue, X. D. Zhang, and J. H. Song, Appl. Phys. Lett. **83**, 1689 (2003).
[2]M. H. Huang, Y. Wu, H. Feick, N. Tran, E. Weber, and P. Yang, Adv. Mater. (Weinheim, Ger.) **13**, 113 (2001).
[3]J.-J. Wu and S.-C. Liu, Adv. Mater. (Weinheim, Ger.) **14**, 215 (2002).
[4]Z. W. Pan, Z. R. Dai, and Z. L. Wang, Science **291**, 1947 (2001).
[5]C. C. Lin, H. P. Chen, H. C. Liao, and S. Y. Chen, Appl. Phys. Lett. **86**, 183103 (2005).
[6]E. G. Bylander, J. Appl. Phys. **49**, 1188 (1978).
[7]D. Li, Y. H. Leung, A. B. Djurisic, Z. T. Liu, M. H. Xie, S. L. Shi, S. J. Xu, and W. K. Chan, Appl. Phys. Lett. **85**, 1601 (2004).
[8]K. Song and S. Lee, Curr. Appl. Phys. **1**, 169 (2001).
[9]Y. Jiang, X. M. Meng, J. Liu, Z. R. Hong, C. S. Lee, and S. T. Lee, Adv. Mater. (Weinheim, Ger.) **15**, 1195 (2003).
[10]H. Masuda and M. Satoh, Jpn. J. Appl. Phys., Part 2 **35**, L126 (1996).
[11]C. A. Dyke, M. P. Stewart, and J. M. Tour, J. Am. Chem. Soc. **127**, 4497 (2005).
[12]R. J. Collins, I. T. Bae, D. A. Scherson, and C. N. Sukenik, Langmuir **12**, 5509 (1996).
[13]H. Tachibana, Y. Yamanaka, H. Sakai, M. Abe, and M. Matsumoto, Chem. Mater. **12**, 854 (2000).
[14]J. A. Rodriguez, T. Jirsak, S. Chaturvedi, and M. Kuhn, Surf. Sci. **442**, 400 (1999).
[15]T. Vdovenkova, A. Vdovenkov, and R. Tornqvist, Thin Solid Films **343**, 332 (1999).
[16]M. Chen, X. Wang, Y. H. Yu, Z. L. Pei, X. D. Bai, C. Sun, R. F. Huang, and L. S. Wen, Appl. Surf. Sci. **158**, 134 (2000).
[17]X. Wang, P. Gao, J. Li, C. J. Summer, and Z. L. Wang, Adv. Mater. (Weinheim, Ger.) **14**, 1732 (2002).
[18]T. W. Kim, T. Kawazoe, S. Yamazaki, M. Ohtsu, and T. Sekiguchi, Appl. Phys. Lett. **84**, 3358 (2004).